

Dwarf carbon stars are likely metal-poor binaries and unlikely hosts to carbon planets

L. J. Whitehouse,¹★ J. Farihi,¹ P. J. Green,² T. G. Wilson¹ and J. P. Subasavage^{3,4}¹University College London, London, WC1E 6BT, UK²Harvard-Smithsonian Center for Astrophysics, 60 Garden St, Cambridge, MA 02138, USA³The Aerospace Corporation, 2310 E. El Segundo Boulevard, El Segundo, CA 90245, USA⁴United States Naval Observatory, 10391 W. Naval Observatory Rd., Flagstaff, AZ 86001-8521, USA

Accepted 2018 June 9. Received 2018 June 07; in original form 2018 April 23

ABSTRACT

Dwarf carbon stars make up the largest fraction of carbon stars in the Galaxy with ≈ 1200 candidates known to date primarily from the Sloan Digital Sky Survey. They either possess primordial carbon-enhancements, or are polluted by mass transfer from an evolved companion such that C/O is enhanced beyond unity. To directly test the binary hypothesis, a radial velocity monitoring survey has been carried out on 28 dwarf carbon stars, resulting in the detection of variations in 21 targets. Using Monte Carlo simulations, this detection fraction is found to be consistent with a 100 per cent binary population and orbital periods on the order of hundreds of days. This result supports the post-mass transfer nature of dwarf carbon stars, and implies they are not likely hosts to carbon planets.

Key words: binaries: general – stars: chemically peculiar – stars: carbon.

1 INTRODUCTION

Carbon stars were historically thought to lie on the asymptotic giant branch (AGB), having dredged up triple- α burning products to their surface. This gives rise to distinct atmospheric chemistry when the C/O ratio exceeds unity, revealing strong molecular absorption bands of C₂, CH, and CN. Intriguingly, it is now known that dwarf stars can exhibit the same distinct absorption features, thus indicating that there exists a carbon-enriched, main-sequence stellar population.

The first dwarf carbon (dC) star discovered was G77-61, a $T_{\text{eff}} \approx 4100$ K, high proper-motion star that was at first assumed to be an M dwarf. A discrepancy was noticed when the $M_V = +10.08$ mag derived from parallax measurements was compared to the observed colour, with the star appearing far redder than expected. Spectroscopy revealed strong molecular carbon features, typical of classical carbon giants, were responsible for the red colour (Dahn et al. 1977) and established the first known main-sequence star with distinct C₂ absorption bands.

Stellar evolution does not predict the synthesis of carbon in single stars until the AGB, resulting in two possible explanations for the atmospheric chemistry of G77-61. The first hypothesis is that the star was formed in a carbon-enriched environment, and the second is that mass was transferred from an evolved companion (now unseen; Dahn et al. 1977). Radial velocity monitoring of G77-61 over a baseline of 3 yr revealed variations consistent with a circular orbit

and 245 d period (Dearborn et al. 1986). The mass function indicated the unseen component must have a mass of at least $0.55M_{\odot}$, consistent with a white dwarf.

Carbon is produced via the triple- α process through helium shell burning on the AGB. This material is then mixed into the envelope raising the carbon abundance over time via a series of convection and pulsation episodes, with the largest being the third dredge-up. This process can produce a C/O ratio well above unity for stars of intermediate mass (Iben & Renzini 1983). If the star is part of a binary, then this carbon-rich material can be transferred to the companion via Roche lobe overflow or efficient wind capture. However, the mass transfer mechanism is currently unconstrained for dC stars owing to the lack of information on orbital separations.

Mass transfer of carbon-rich material from an AGB star is widespread amongst binary systems, with other well-known examples being carbon-enhanced, metal-poor s-type (CEMP-s), Ba, and CH stars. CEMP-s stars are defined by their relatively low metallicity, high carbon abundance, and high abundance of Ba ($[\text{Fe}/\text{H}] < -2.0$, $[\text{C}/\text{Fe}] > +1.0$, $[\text{Ba}/\text{Fe}] > +1.0$; Aoki et al. 2007), whereas Ba and CH stars are more loosely defined as containing strong absorption features of Ba and CH, respectively. These stars are typically giants with Ba and CH stars found in the red clump and on the main-sequence turn-off, respectively (Escorza et al. 2017), while CEMP-s stars populate the first ascent giant branch (RGB). All three populations exhibit radial velocity variations consistent with high binary fractions and orbital periods typically on the order of hundreds to thousands of days (McClure & Woodsworth 1990; Jorissen et al. 1998; Hansen et al. 2016).

★ E-mail: lewis.whitehouse.16@ucl.ac.uk

In this paper, the first results of a radial velocity monitoring survey are presented for 28 dC stars. The results to date are consistent with a binary fraction possibly as high as 100 per cent, supporting a post-mass transfer origin. In Section 2, the target selection and observations are described, with the results given in Section 3. The results are discussed in Section 4, with the preliminary conclusions presented in Section 5.

2 TARGET SELECTION AND OBSERVATIONS

Potential targets were compiled from the literature based on brightness, and selected to have a high likelihood of being a main-sequence star. The bulk of potential targets were found within the Sloan Digital Sky Survey (SDSS), with the first few hundred candidates identified via colour cuts (Downes et al. 2004). The largest sample of dC candidates to date was later discovered via cross-correlation to template spectra in DR7 and DR8 (Green 2013). Additional dC stars identified via colour and proper motion were also included among potential targets (Liebert et al. 1994; Totten, Irwin & Whitelock 2000; Lowrance et al. 2003; Rossi et al. 2011), including the prototype G77-61. From an initial pool of 73 potential targets brighter than $g = 19.0$ AB mag, roughly three dozen stars have been observed at least once, and the 28 targets with two or more observations are listed in Table 1.

The observations were carried out using the ISIS spectrograph on the William Herschel Telescope at Roque de los Muchachos. The data reported here were obtained between 2013 February and 2017 August, using the ISIS blue arm and the EEV12 detector with no dichroic. The R1200B grating and a 1 arcsec slit were used to achieve a resolving power $R \approx 6400$ over the range 5000–6000 Å. This choice was motivated by the presence of several strong absorption features for robust cross-correlation, with the region including the C₂ Swan bands at 5165 and 5636 Å, the Mg I triplet at 5183 Å, and the Na I doublet at 5889 Å. The spectral coverage achieved with ISIS and the above settings is plotted in Fig. 1. Observations were taken at airmasses below 1.5, and using individual exposure times between 300 and 1200 s, with a goal signal-to-noise ratio (S/N) > 10. Three or more exposures were taken for each target per observation, to increase S/N, and to minimise the effect of cosmic rays and detector artifacts.

To obtain reliable wavelength solutions, arc lamps were observed for 60 s immediately before and after each set of science exposures thus correcting any flexure in the optics between pointings. The CuNe+CuAr lamps were chosen for calibration owing to the high number of features in the designated spectral range. Individual arcs were then cross-identified against a master arc frame that consisted of several exposures taken at the start of the night at zenith.

3 REDUCTION AND ANALYSIS

3.1 Data reduction and binary fraction

The spectral images were trimmed, bias subtracted, and flat fielded using standard routines in IRAF.¹ Individual spectra were extracted using the APALL package and then combined as a weighted mean to facilitate the removal of cosmic rays and increase S/N. The wavelength calibration for each combined spectrum was obtained by

taking the average wavelength solution for the arc frames taken directly before and after the science exposure. Subsequently each target was flux calibrated using a suitable standard star with few absorption lines over the observed spectral range.

Radial velocity variations were evaluated using the package FXCOR that performs a Fourier cross-correlation between an input spectrum and a given template (Tonry & Davis 1979). For each target, the highest S/N spectrum was chosen as a template against which all other observations were cross-correlated (Marsh, Robinson & Wood 1994). The velocity residuals (in km s⁻¹) of the cross-correlation were added in quadrature to the velocity uncertainty from wavelength calibration, yielding a total error for each pair of spectra. This total error depends on the S/N of the target, with higher S/N targets possessing errors < 1 km s⁻¹ and lower S/N targets exhibiting errors up to 6 km s⁻¹, but typically less than a few km s⁻¹. Only relative radial velocities were determined in this study, as individual molecular transitions depend on gas temperature and pressure. Due to the presence of only a few atomic lines in the spectra, absolute radial velocities will be derived and presented in a forthcoming paper.

A weighted χ^2 test was used to determine if any velocity variation could be due to the measurement errors (Lucatello et al. 2005; Starkenburg et al. 2014). The results of the weighted χ^2 test are given in Table 1, where $p(\chi^2|\nu)$ is the probability that the observed radial velocity variations are real given the errors, and ν is the number of degrees of freedom (which here is the number of observations). A small p value thus indicates a low probability that the null hypothesis of constant radial velocity can be accepted, implying the system is likely binary.

A limit of $\log_{10}(p) < -2$ (less than 1 chance in 100) was used to reject the null hypothesis that a target was not radial velocity variable. By this definition, 21 of the 28 targets are consistent with being radial velocity variable. Despite prior knowledge that G77-61 and PG 0824 + 288 are binary (Dearborn et al. 1986; Heber et al. 1993), both were included in the statistics as the sample was selected for brightness and visibility. No radial velocity variations were detected in PG 0824 + 288, but this is unsurprising given the fact it was spatially resolved at ≈ 17 au (corresponding to an orbital period of $\gtrsim 60$ yr; Farihi, Hoard & Wachter 2010). The binary detection rate is therefore 75 per cent.

3.2 Simulations

To numerically constrain the survey sensitivity, a set of Monte Carlo simulations was run for a model population of dC stars. The simulation was run for 10 000 stars with an initial binary fraction of 60 per cent, consistent with field stars brighter than $M_v \approx +8$ mag within 25 pc (Jahreiß & Wielen 2000), while varying the orbital parameters. The number of radial velocity measurements for each simulated star was chosen randomly between 2 and 8 to be consistent with the sampling of the survey. Each set of modelled radial velocities were then analysed using the same method adopted for the empirical data to derive a p value, where errors were randomly assigned to each modelled radial velocity measurement with magnitudes comparable to the total errors in the survey. To measure the sensitivity, the same $\log_{10}(p) < -2$ detection criteria was applied.

Orbital parameters for each simulated binary system were assigned randomly, with inclination angle, argument of pericenter, and pericenter phase, all being assigned from uniform distributions. The mass of each simulated dC star was sampled from a Salpeter initial mass distribution (Salpeter 1955) with upper and lower bounds set at $0.8M_{\odot}$ and $0.2M_{\odot}$ respectively, based on masses of K and

¹IRAF is distributed by the National Optical Astronomy Observatory, which is operated by the Association of Universities for Research in Astronomy under a cooperative agreement with the National Science Foundation.

Table 1. Dwarf carbon stars observed during the radial velocity monitoring survey with at least two observations. Column six shows the p value of each target expressed logarithmically with an arbitrary lower limit placed at $\log_{10}(p) = -6.0$, corresponding to a 10^{-6} chance of a target being non-binary. The seventh column gives the maximum radial velocity difference between any two sets of observations, and in the eighth column this is divided by the largest error in relative radial velocity, and is thus a measure of the statistical significance.

Name	RA	Dec	Epochs	Baseline (d)	$\log_{10}(p)$	$\Delta v_{\text{rad, max}}$ (km s $^{-1}$)	Significance (σ)
LHS 1075	00 26 00.48	-19 18 52.0	6	1469	<-6.0	26.0	5.3
SDSS J012028	01 20 28.56	-08 36 30.9	5	1469	-3.0	22.4	5.1
SDSS J012150	01 21 50.42	+01 13 01.4	5	1469	<-6.0	71.2	15.3
SDSS J013007	01 30 07.13	+00 26 35.3	5	1469	-3.6	28.3	3.8
SDSS J022304	02 23 04.43	+00 45 01.3	5	1652	-2.5	20.2	4.8
G77-61 ^a	03 32 38.08	+01 58 00.0	8	1651	<-6.0	28.9	4.4
SDSS J074257 ^a	07 42 57.17	+46 59 17.9	5	1037	-1.0	7.2	2.9
SDSS J081157	08 11 57.14	+14 35 33.0	6	1059	-4.6	23.5	3.9
PG 0824+288	08 27 05.09	+28 44 02.4	5	1059	-0.1	8.3	1.1
C 0930-00	09 33 24.64	-00 31 44.5	6	1061	-3.9	22.4	5.5
SDSS J093334	09 33 34.14	+06 48 12.6	4	677	-2.6	16.9	5.0
SDSS J095545	09 55 45.84	+44 36 40.4	4	1061	-5.3	32.6	5.6
SDSS J101548	10 15 48.90	+09 46 49.7	2	388	-3.3	26.2	6.8
SDSS J110458	11 04 58.97	+27 43 11.8	3	1059	-0.0	0.9	0.1
KA 2	11 19 03.90	-16 44 49.3	2	5	<-6.0	70.5	20.5
SDSS J112633	11 26 33.94	+04 41 37.7	2	5	-0.4	11.0	1.4
SDSS J120024	12 00 24.09	+38 17 20.3	2	1	-0.3	4.1	1.1
CLS 50	12 20 00.77	+36 48 01.7	4	763	<-6.0	40.3	7.9
SDSS J130744	13 07 44.53	+60 09 03.7	3	1651	-0.7	9.8	1.8
SBS 1310+561	13 12 42.51	+55 55 54.6	6	1651	<-6.0	32.3	7.2
SDSS J145725	14 57 25.86	+23 41 25.4	5	1469	-1.3	20.1	4.9
CBS 311	15 19 05.99	+50 07 02.8	4	579	<-6.0	46.8	4.2
CLS 96	15 52 37.35	+29 27 59.1	5	1469	-4.7	11.0	5.9
LP 225-12 ^a	16 22 32.86	+42 37 54.2	6	1469	<-6.0	30.8	3.9
SDSS J184735	18 47 35.67	+40 59 44.1	4	1469	<-6.0	25.2	6.7
LSR J2105+2514	21 05 16.54	+25 14 48.6	6	1469	<-6.0	122.4	27.9
LP 758-43 ^a	21 49 37.84	-11 38 28.5	6	1469	<-6.0	29.2	3.3
SDSS J235443	23 54 43.13	+36 29 07.1	5	1030	-4.7	34.2	6.7

Note: ^a These four targets possess orbital periods constrained in the literature.

M dwarfs. Each white dwarf mass was sampled from a normal distribution with $M_* = 0.63M_{\odot} \pm 0.14$ (Tremblay et al. 2016).

Initially, the simulated orbital period distribution was set to $\log_{10}T$ (d) = 4.8 ± 2.3 (based on radial velocity studies of G dwarfs; Duquennoy & Mayor 1991). The orbital eccentricity was assigned depending on the period, with $e = 0$ for $T < 1000$ d, and longer periods taken from a normal distribution $e = 0.4 \pm 0.2$. A maximum orbital period of 10 000 yr ($\log_{10}T$ (d) = 6.6) was adopted as systems with excessively long periods would not be detected given the baseline of the survey. Sampling the aforementioned orbital period distribution, which has a 60 per cent binary fraction, resulted in a simulated detection rate of just 16 per cent. Increasing the binary fraction to 100 per cent raised the simulated detection rate to 27 per cent, still far below the observational detection rate of 75 per cent. Thus, the orbital period distribution of nearby G dwarfs appears to be highly discrepant with the dC star population.

The Monte Carlo simulations were rerun using shorter orbital period distributions to better replicate the observed detection rate. In order to increase the simulated detection rate, circular orbits were adopted as these yielded more detections than eccentric orbits (by ≈ 2 per cent), and only populations with 100 per cent binary fractions were simulated. A distribution of $\log_{10}T$ (d) = 3.6 ± 1.8 was tried as this represents a reasonable approximation of the periods observed for Ba, CH, and CEMP-s stars (Jorissen et al. 1998, 2016; Hansen et al. 2016). This yielded a simulated detection rate of 37 per cent and still falls significantly short of the detected rate.

Shorter orbital period distributions were then explored by decreasing the mean of the log-normal distribution in steps of 0.2 dex. The standard deviation of the distribution was initially set at one half the value of the mean, and then decreased in steps of 0.1 dex. This method was carried out until the simulated detection rate converged closest to that observed. While there is no unique period distribution that best approximates the detected binary fraction, a good representative distribution is $\log_{10}T$ (d) = 2.0 ± 0.8 , and yields a simulated detection rate of 72 per cent. Most targets show $\Delta v_{\text{rad, max}}$ on the order of 20 – 40 km s $^{-1}$, thus consistent with orbital periods of hundreds to thousands of days. Therefore, both the simulations and the observed changes in radial velocities both provide consistent orbital period range estimates.

If the dC star population is 100 per cent binary, then the targets that do not show sufficient radial velocity variations are therefore probably either long period binaries or low inclination systems that would yield small velocity semi-amplitudes. Because two stars (SDSS J112633 and SDSS J120024) were only observed twice each, and with a baseline of less than 5 d each, there is a wide range of orbital periods that could not be detected for these targets. The remaining four null-detections (SDSS J074257, SDSS J110458, SDSS J130744, and SDSS J145725) have a baseline of over 3 yr, possibly suggesting inclinations that are close to pole-on. Additional data are required to determine the exact orbital parameters, because the bulk of targets have an insufficient number of observations.

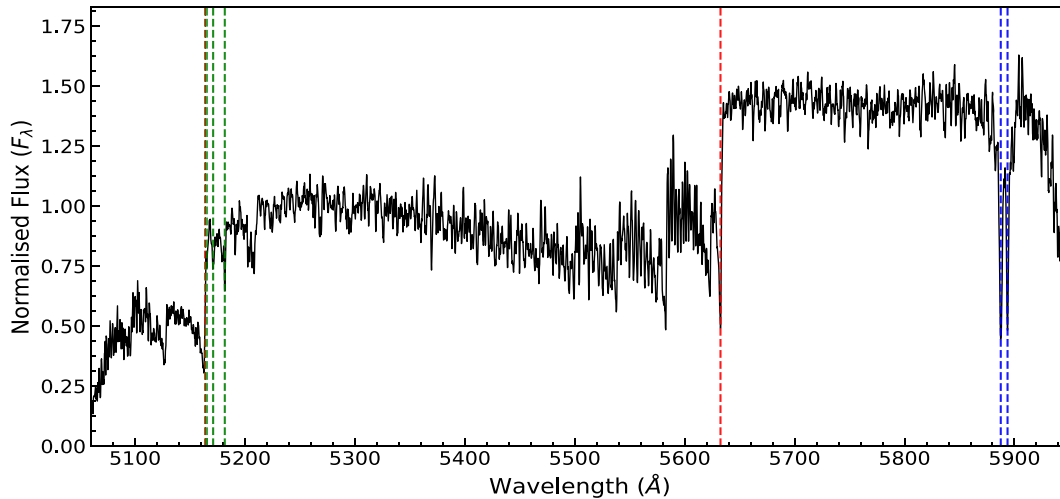


Figure 1. The combined ISIS spectrum of the target LP 225-12 showing the full spectral range for the adopted instrumental setup, including vignetting towards the end points. The red lines correspond to the C_2 Swan band heads, green corresponds to the $Mg\ I$ triplet, and blue corresponds to the $Na\ I$ D doublet.

4 DISCUSSION

4.1 Binary fraction and orbital evolution

The observed variation in relative radial velocities of dC stars are consistent with the hypothesis that carbon-enhanced material was transferred from an evolved companion. Within the observed sample, 75 per cent show clear variations and are consistent with a 100 per cent binary population. The simulated period distributions that best match the observational detection rate suggest that either Roche lobe overflow or efficient wind capture may be responsible for the observed pollution in dC stars.

To date five bona fide dC stars have determined orbital periods. SDSS J125017 was shown to have 2.9 d periodic variability in its light curve, and this was confirmed to correspond to its orbital period via radial velocity measurements (Margon et al. 2018). Interestingly, in their search of ≈ 1000 dC star light curves using Palomar Transient Factory data, Margon et al. (2018) find only SDSS J125017 exhibited variations consistent with a short period binary. This may indicate that the majority of dC stars do not have short orbital periods and are hence unlikely to be post-common envelope systems. However, the sensitivity to binary-induced photometric variability has yet to be established for dC stars.

Three further dC binary orbital periods have recently been determined astrometrically at the US Naval Observatory (USNO) and lie in the range $\approx 400 - 4000$ d (Harris et al. 2018). This period range is broadly consistent with the distribution adopted in Section 3.2 based on binary simulations that are well-matched to the detected fraction of stars with radial velocity changes. Importantly, all three of these targets have at least five radial velocity observations in this study, and their $\Delta v_{\text{rad, max}}$ values in Table 1 are consistent with Keplerian orbits at their determined inclinations. Thus, the USNO astrometry strengthens the argument that dC stars are likely to typically have orbits on the order of hundreds to thousands of days.

Interestingly, together with G77-61 which possess a period of 245 d (Dearborn et al. 1986), these four dC stars appear to lie in a ‘no man’s land’ for low-mass, unevolved companions to white dwarfs, as theory predicts that any secondary should spiral in or spiral out of this region owing to the effects of mass loss during the AGB (Willems & Kolb 2004). Mass loss can overflow the AGB star Roche lobe and create a common envelope that causes an initially

close companion to inspiral due to friction (Ivanova et al. 2013). In contrast, if the initial binary separation is sufficiently large, then as mass is lost the orbital separation will increase to conserve angular momentum.

These theoretical predictions are strongly confirmed among commonly occurring white dwarf-M dwarf binary systems, where there is a clear dearth of pairs with orbital separations in the region $\sim 1 - 10$ au as established via space-based imaging in the optical (Farihi et al. 2010). In contrast, there are myriad short-period ($\lesssim 10$ d; Rebassa-Mansergas et al. 2008), post-common envelope systems, and long-period ($\gtrsim 50$ yr) widely separated white dwarf-M dwarf systems detected by common-proper motion (Farihi, Becklin & Zuckerman 2005). Comparing the spectral types of M dwarfs in post-common envelope systems to those in widely separated binaries, reveals no obvious differences (Schreiber et al. 2010), therefore suggesting that neither process is capable of efficient mass transfer. This is further supported by the detection of just one dC star among a sample of 1600 white dwarf-red dwarf binaries identified from the SDSS via template matching and identifying excess red fluxes via optical and near-infrared survey data (Rebassa-Mansergas et al. 2010). Though dC stars would not be found via template matching to a white dwarf-red dwarf composite spectrum, it would be expected that binaries identified via a red excess to the white dwarf spectrum could include dC stars. Their rare nature as companions to known white dwarfs is consistent with the fact that only 9 of 1211 SDSS dC stars possess composite spectra.

The results to date from this study indicate that these intermediate orbital periods may be typical for dC stars, and thus are likely a key characteristic tied to their origin. If indeed most dC stars possess periods of hundreds to thousands of days, then they may be similar to those found for Ba, CH, and CEMP-s stars (Pols et al. 2003; Izzard et al. 2010). Furthermore, the similarities between these polluted systems extends to metallicity, with all three populations metal-deficient with respect to solar, most notably the CEMP-s stars. High-resolution spectroscopy has revealed G77-61 is one of the most metal-poor stars known ($[Fe/H] = -4.0$; Plez & Cohen 2005), and preliminary kinematical results based on *Gaia* DR1 suggest that the dC population as a whole are old and metal-poor, with roughly 30 – 60 per cent halo members (Farihi et al. 2018). Thus it appears that metal-poverty is important for C/O enhancement in dC stars.

4.2 Carbon chemistry exoplanets

There has been considerable interest in the existence of exoplanets that exhibit carbon dominated chemistry (Madhusudhan et al. 2011). The existence of such planets requires that the protoplanetary material be intrinsically enriched in carbon such that $C/O > 0.8$ (Bond, O'Brien & Lauretta 2010). In this scenario, major planet-building materials could be predominantly carbide minerals, allowing for a SiC, TiC, graphite mantle with an Fe–Si–Ni core. Such planets would be chemically distinct from the rocky bodies found within the solar system. Although unrelated to the present study, it is noteworthy that the minor bodies that pollute the surfaces of white dwarf stars exhibit Earth-like or chondritic C/O , with no evidence for carbon-dominated materials (Wilson et al. 2016).

The potential frequency of carbon-rich exoplanets depends on the space density of viable host stars (Fortney 2012). While dC stars are the most numerous carbon stars in the Galaxy, they are still far less abundant than their oxygen-rich counterparts, with approximately 1:650 000 dC stars relative to low-mass K and M dwarfs ($0.1M_{\odot} < M < 0.8M_{\odot}$; Bochanski et al. 2010; de Kool & Green 1995). With drastically fewer potential hosts with $C/O > 1$, the expected relative abundance of carbon-rich planets could be vanishing.

Assuming carbon-rich planets can and do form around host stars with $C/O > 0.8$, the results presented here, that all low-mass, main-sequence stars in the phase space above $C/O = 1.0$ are consistent with 100 per cent duplicity, therefore diminishes the possibility of single stars with $C/O \geq 1.0$, and thus their ability to host planets. Thus, the available real estate for carbon planets may be dismal. However, one subgroup of CEMP stars appears to commonly possess both binary and single members (the CEMP-no stars; Starkenburg et al. 2014) and therefore may contain primordial carbon-enhancement. If these stars are formed from carbon-enhanced nebulae, then presumably they are possible sites for carbon-rich planets (Mashian & Loeb 2016), notwithstanding the potentially unfavourable planet hosting frequency of metal-poor stars (Fischer & Valenti 2005).

5 CONCLUSIONS

This radial velocity monitoring survey shows that 21 of 28 (75 per cent) dC stars exhibit radial velocity variations consistent with duplicity. Using Monte Carlo simulations for a 100 per cent binary population with an orbital period distribution $\log_{10} T(d) = 2.0 \pm 0.8$, the empirical (75 per cent) and predicted (72 per cent) detection rates are well matched. Thus, the dC stars appear consistent with a 100 per cent binary population, supporting the post-mass transfer nature of these stars. When compared to white dwarf-M dwarf binaries, which exhibit a bimodal period distribution, the dC population appears to lie between the peaks, indicating that efficient mass transfer circumvents migration to short or long periods.

The high binary fraction of dC stars constrains the potential real estate for carbon-rich exoplanets, owing to the extrinsic nature of their high carbon abundance. As dC stars are the product of efficient mass transfer, the chemistry of the system during the planet formation phase would not reflect the chemistry of the dC star observed today. This may also be true for all main-sequence stars that exhibit C/O significantly above solar; if they exist (which is uncertain; Fortney 2012; Teske et al. 2014) such stars could be the result of binary mass transfer. It is clear from the dC stars that carbon enhancement in a main-sequence star is possible via binary evolution, and thus

more subtle C/O enhancements may be more common (e.g. in FGK stars).

Continued radial velocity measurements for the stars in this study are necessary to determine actual orbits. Physical models of mass transfer – for example Roche lobe overflow or wind capture (Paczýński 1965; Abate et al. 2015) – can only be tested with tightly constrained binary periods. State-of-the-art mass transfer models currently face challenges in producing carbon-enhanced stars in general (Izzard et al. 2010; Matrozos, Abate & Stancliffe 2017), and the newly uncovered dC binary population can provide an additional and distinct set of empirical constraints.

ACKNOWLEDGEMENTS

The authors would like to thank H. C. Harris, B. T. Gänsicke, I. D. Howarth, and an anonymous reviewer for feedback that improved the quality of the manuscript. The data obtained in this paper was done so using the William Herschel Telescope that is operated on the island of La Palma by the Isaac Newton Group of Telescopes in the Spanish Observatorio del Roque de los Muchachos of the Instituto de Astrofísica de Canarias.

REFERENCES

- Abate C., Pols O. R., Stancliffe R. J., Izzard R. G., Karakas A. I., Beers T. C., Lee Y. S., 2015, *A&A*, 581, A62
- Aoki W., Beers T. C., Christlieb N., Norris J. E., Ryan S. G., Tsangarides S., 2007, *ApJ*, 655, 492
- Bochanski J. J., Hawley S. L., Covey K. R., West A. A., Reid I. N., Golimowski D. A., Ivezić Ž., 2010, *AJ*, 139, 2679
- Bond J. C., O'Brien D. P., Lauretta D. S., 2010, *ApJ*, 715, 1050
- Dahn C. C., Liebert J., Kron R. G., Spinrad H., Hintzen P. M., 1977, *ApJ*, 216, 757
- de Kool M., Green P. J., 1995, *ApJ*, 449, 236
- Dearborn D. S. P., Liebert J., Aaronson M., Dahn C. C., Harrington R., Mould J., Greenstein J. L., 1986, *ApJ*, 300, 314
- Downes R. A. et al., 2004, *AJ*, 127, 2838
- Duquennoy A., Mayor M., 1991, *A&A*, 248, 485
- Escorza A. et al., 2017, *A&A*, 608, A100
- Farihi J., Becklin E. E., Zuckerman B., 2005, *ApJS*, 161, 394
- Farihi J., Hoard D. W., Wachter S., 2010, *ApJS*, 190, 275
- Farihi J., Arendt A. R., Machado H. S., Whitehouse L. J., 2018, *MNRAS*, 477, 3801
- Fischer D. A., Valenti J., 2005, *ApJ*, 622, 1102
- Fortney J. J., 2012, *ApJ*, 747, L27
- Green P., 2013, *ApJ*, 765, 12
- Hansen T. T., Andersen J., Nordström B., Beers T. C., Placco V. M., Yoon J., Buchhave L. A., 2016, *A&A*, 588, A3
- Harris H. C., et al., 2018, *AJ*, 155, 252
- Heber U., Bade N., Jordan S., Voges W., 1993, *A&A*, 267, L31
- Iben I., Jr, Renzini A., 1983, *ARA&A*, 21, 271
- Ivanova N. et al., 2013, *A&AR*, 21, 59
- Izzard R. G., Dermine T., Church R. P., 2010, *A&A*, 523, A10
- Jahreiß H., Wielen R., 2000, in Reipurth B., Zinnecker H., eds, Proc. IAU Symp. 200, The Census of Nearby Stars Binaries, Potsdam, Germany, p. 129
- Jorissen A. et al., 2016, *A&A*, 586, A158
- Jorissen A., Van Eck S., Mayor M., Udry S., 1998, *A&A*, 332, 877
- Liebert J., Schmidt G. D., Lesser M., Stepanian J. A., Lipovetsky V. A., Chaffe F. H., Foltz C. B., Bergeron P., 1994, *ApJ*, 421, 733
- Lowrance P. J., Kirkpatrick J. D., Reid I. N., Cruz K. L., Liebert J., 2003, *ApJ*, 584, L95
- Lucatello S., Tsangarides S., Beers T. C., Carretta E., Gratton R. G., Ryan S. G., 2005, *ApJ*, 625, 825

- Madhusudhan N., Mousis O., Johnson T. V., Lunine J. I., 2011, *ApJ*, 743, 191
- Margon B., Kupfer T., Burdge K., Prince T. A., Kulkarni S. R., Shupe D. L., 2018 *ApJ*, 856, L2
- Marsh T. R., Robinson E. L., Wood J. H., 1994, *MNRAS*, 266, 137
- Mashian N., Loeb A., 2016, *MNRAS*, 460, 2482
- Matrozis E., Abate C., Stancliffe R. J., 2017, *A&A*, 606, A137
- McClure R. D., Woodsworth A. W., 1990, *ApJ*, 352, 709
- Paczyński B., 1965, *AcA*, 15, 89
- Plez B., Cohen J. G., 2005, *A&A*, 434, 1117
- Pols O. R., Karakas A. I., Lattanzio J. C., Tout C. A., 2003, in Corradi R. L. M., Mikolajewska J., Mahoney T. J., eds, *ASP Conf. Ser. Vol. 303, Symbiotic Stars Probing Stellar Evolution*, Astron. Soc. Pac., San Francisco, p. 290
- Rebassa-Mansergas A. et al., 2008, *MNRAS*, 390, 1635
- Rebassa-Mansergas A., Gänsicke B. T., Schreiber M. R., Koester D., Rodríguez-Gil P., 2010, *MNRAS*, 402, 620
- Rossi C., Gigoyan K. S., Avtandilyan M. G., Sclavi S., 2011, *A&A*, 532, A69
- Salpeter E. E., 1955, *ApJ*, 121, 161
- Schreiber M. R. et al., 2010, *A&A*, 513, L7
- Starkenburger E., Shetrone M. D., McConnachie A. W., Venn K. A., 2014, *MNRAS*, 441, 1217
- Teske J. K., Cunha K., Smith V. V., Schuler S. C., Griffith C. A., 2014, *ApJ*, 788, 39
- Tonry J., Davis M., 1979, *AJ*, 84, 1511
- Totten E. J., Irwin M. J., Whitelock P. A., 2000, *MNRAS*, 314, 630
- Tremblay P.-E., Cummings J., Kalirai J. S., Gänsicke B. T., Gentile-Fusillo N., Raddi R., 2016, *MNRAS*, 461, 2100
- Willems B., Kolb U., 2004, *A&A*, 419, 1057
- Wilson D. J., Gänsicke B. T., Farihi J., Koester D., 2016, *MNRAS*, 459, 3282

This paper has been typeset from a $\text{\TeX}/\text{\LaTeX}$ file prepared by the author.